CIRCUITS SYSTEMS SIGNAL PROCESS
VOL. 14, NO. 4, 1995, PP. 539–553

NEW TIME-FREQUENCY DISTRIBUTION*

Soo-Chang Pei[1] *and Er-Jung Tsai*[1]

Abstract. Cross terms are an inherent consequence of the second order nature of Cohen's class TFDs (Time-Frequency Distributions) [5], [6]. They are manifest in a TFD of multi-component signals as spurious artifacts arising from interactions between the various signal components, and they can often appear at times and/or frequencies inconsistent with the underlying physical nature of the signal, causing misinterpretation [2], [3], [4]. There are many time frequency distributions that avoid the cross term effect; the best are the Choi-Williams ED (Exponential Distribution) [1] and Levin's IPS (Instantaneous Power Spectrum) [9]. In this paper we combine the cross term reducing philosophy of the ED and IPS to obtain a new TFD that most effectively reduces the cross term effect. Surprisingly, the new TFD also satisfies most desired TFD properties.

1. Introduction

Cross terms are an inherent consequence of the second order nature of Cohen's class TFDs. They are manifest in a TFD of multi-component signals as spurious artifacts arising from interactions between the various signal components, and they can often appear at times and/or frequencies inconsistent with the underlying physical nature of the signal, causing misinterpretations.

Generally speaking, there are two alternative methods for controlling cross term interference.

(1) Interference attenuation: One example, the Choi-Williams ED [1], effectively attenuates cross interference and also satisfies many desirable properties of TFDs.

(2) Interference concentration: As an example, Levin's IPS [9] produces cross terms only at signal frequencies, and only during time intervals in which the signal is nonzero.

* Received February 12, 1993; accepted November 22, 1993.

[1] Institute of Electrical Engineering, National Taiwan University, Taipei, Taiwan, Republic of China.

In this paper we will promote a new TFD that not only can meet interference attenuation constraints, but can also approximately satisfy interference concentration constraints including many useful TFD properties [6], [7], and [10].

2. Design philosophy

First, we recall the definition of Cohen's class [5] for signal $s(t)$:

$$P(t,\omega) = \frac{1}{2\pi}\int\int\int e^{-j\theta t - j\omega\tau + j\theta\mu}\phi(\theta,\tau) \cdot s\left(\mu+\frac{1}{2}\tau\right)s^*\left(\mu-\frac{1}{2}\tau\right)d\mu\,d\tau\,d\theta \tag{1}$$

$$= \frac{1}{2\pi}\int\int\psi(t-\mu,\tau)s\left(\mu+\frac{1}{2}\tau\right)s^*\left(\mu-\frac{1}{2}\tau\right)e^{-j\omega\tau}d\mu\,d\tau \tag{2}$$

$$= \frac{1}{4\pi^2}\int\int\varphi(\theta,\omega-\eta)S^*\left(\eta+\frac{1}{2}\theta\right)S\left(\eta-\frac{1}{2}\theta\right)e^{-j\theta t}d\eta\,d\theta \tag{3}$$

$$= \int\int\phi(\theta,\tau)A_s(\theta,\tau)e^{-j\theta t-j\omega\tau}d\theta\,dt\,, \tag{4}$$

where

$$S(\omega) = \int s(t)e^{-j\omega t}dt \tag{5}$$

$$\psi(\mu,\tau) = \int \phi(\theta,\tau)\,e^{-j\theta\mu}d\theta \tag{6}$$

$$\varphi(\theta,\eta) = \int \phi(\theta,\tau)\,e^{-j\eta\tau}d\tau \tag{7}$$

and

$$A_s(\theta,\tau) = \frac{1}{2\pi}\int s\left(\mu+\frac{1}{2}\tau\right)s^*\left(\mu-\frac{1}{2}\tau\right)e^{j\theta\mu}d\mu\,. \tag{8}$$

$A_S(\theta,\tau)$ is the ambiguity function of $s(t)$ and $\phi(\theta,\tau)$ is an arbitrary function called the kernel function by Classen [4]. The kernel function of Cohen's class is the key to properties of TFDs. The properties of TFDs can correspond to constraints on the kernel function [6], [10], and [11].

Flandrin [7] pointed out that the desired components of the ambiguity function fall along the θ,τ axes in the (θ,τ) plane. Thus, the interference attenuation constraint requires that

$$\phi(\theta,\tau) \text{ is low-pass in } (\theta,\tau)\,. \tag{9}$$

Loughlin et al. [10] pointed out that the constraints on $\phi(\theta,\tau)$ for preventing cross terms from appearing at nonsignal frequencies and appearing in time intervals

where the signal is zero in the TFD are

$$\varphi(\theta, \eta) = 0\,, \quad \text{for} \quad |\eta| \neq \frac{1}{2}|\theta|\,, \tag{10}$$

$$\psi(\mu, \tau) = 0\,, \quad \text{for} \quad |\mu| \neq \frac{1}{2}|\tau|\,. \tag{11}$$

Equations (10) and (11) are the interference concentration constraints.

Interestingly, the kernel function of the ED [1],

$$\phi_{\text{ED}}(\theta, \tau) = e^{-\frac{\theta^2\tau^2}{\sigma}} \tag{12}$$

strongly satisfies the interference attenuation constraint (9), and the kernel function of the IPS [9]

$$\phi_{\text{IPS}}(\theta, \tau) = \cos\left(\frac{1}{2}\theta\tau\right) \tag{13}$$

meets the interference concentration constraints (10) and (11). Now, we think about a kernel function equal to the product of the ED's and IPS's kernel functions. Will the new TFD have a strong anti-interference effect? We will prove that the new TFD not only has the least interference effect but also meets useful TFD properties.

3. The new TFD

We define the kernel function of the new TFD to be the product of the ED [1] and IPS [9],

$$\phi_{\text{NEW}}(\theta, \tau) = e^{-\frac{\theta^2\tau^2}{\sigma}} \cos\left(\frac{1}{2}\theta\tau\right)\,, \tag{14}$$

in which the former is famous for interference attenuation and the latter is well known for interference concentration. The other form of kernel function can be expressed by

$$\psi_{\text{NEW}}(\mu, \tau) = \frac{1}{2}\frac{\sqrt{\pi\sigma}}{\tau}\left[e^{-\frac{(\mu+\tau/2)^2}{4\tau^2/\sigma}} + e^{-\frac{(\mu-\tau/2)^2}{4\tau^2/\sigma}}\right]\,, \tag{15}$$

$$\varphi_{\text{NEW}}(\theta, \eta) = \frac{1}{2}\frac{\sqrt{\pi\sigma}}{\theta}\left[e^{-\frac{(\eta+\theta/2)^2}{4\theta^2/\sigma}} + e^{-\frac{(\eta-\theta/2)^2}{4\theta^2/\sigma}}\right]\,. \tag{16}$$

From these alternative kernel forms, we can get the properties of the new TFD [6], [7], and [10]. In Table 1 we list some famous TFDs. In Table 2 we compare the properties of the new TFD with other famous TFDs. Although it is impossible to satisfy all the desirable properties of a TFD because of trade-offs, we have already made the new distribution meet various requirements as much as possible.

Table 1. Some popular distributions and their kernels.

TFD	Kernel $\phi(\theta, \tau)$	Formulation $P(t, \omega)$
Page [11]	$e^{j\theta\lvert\tau\rvert/2}$	$\frac{\partial}{\partial t}\left\lvert\int_{-}^{t} s(t')e^{-j\omega t}dt'\right\rvert^2$
Levin's IPS [9]	$\cos\left(\frac{1}{2}\theta\tau\right)$	$\mathrm{Re}\, s(t)S^*(\omega)e^{-j\omega\tau}$
Kirkwood [8]	$e^{j\theta\tau/2}$	$s(t)S^*(\omega)e^{-j\omega\tau}$
Spectrogram	$\int h\left(\mu+\frac{1}{2}\tau\right)h^* \cdot\left(\mu-\frac{1}{2}\tau\right)e^{-j\theta\mu}d\mu$	$\left\lvert\int s(\tau)h(\tau-t)e^{-j\omega\tau}d\tau\right\rvert^2$
WVD, Wigner [13], Ville [12]	1	$\int s\left(t+\frac{1}{2}\tau\right)s^* \cdot\left(t-\frac{1}{2}\tau\right)e^{-j\omega\tau}d\tau$
Choi-Williams ED [1]	$e^{-\theta^2\tau^2/\sigma}$	$\int\int\sqrt{\frac{\sigma}{4\pi\tau^2}}e^{-\frac{(\mu-\tau)^2}{4\tau^2/\sigma}}s\left(\mu+\frac{1}{2}\tau\right) \cdot s^*\left(\mu-\frac{1}{2}\tau\right)e^{-j\omega\tau}d\mu\, d\tau$

Table 2. Some popular distributions and their properties.

	IPS	Spectrogram	WVD	ED	New TFD
Shift-invariant	*	*	*	*	*
Reality	*	*	*	*	*
Scale-invariant	*		*	*	*
Marginal	*		*	*	*
Mean conditional frequency/time	*		*	*	*
Range of distribution	*		*		
Interference attenuation		*		*	*
Interference concentration	*	*			*
Moyal formula			*		
W.S.S. random signal	*		*	*	*

Substituting (14) into (1), we get the definition of the new TFD,

$$P_{\mathrm{NEW}}(\tau,\omega)=\frac{1}{2\pi}\int\int\int e^{-j\theta t-j\omega\tau+j\theta\mu}\,e^{-\frac{\theta^2\tau^2}{\sigma}} \cdot\cos\frac{\theta\tau}{2}s\left(\mu+\frac{1}{2}\tau\right)s^*\left(\mu-\frac{1}{2}\tau\right)d\mu\,d\tau\,d\theta\,. \tag{17}$$

Similarly, expressed in terms of the spectrum,

$$P_{\mathrm{NEW}}(t,\omega)=\frac{1}{4\pi^2}\int\int\int e^{-j\theta t-j\omega\tau+j\tau\mu}\,e^{-\frac{\theta^2\tau^2}{\sigma}} \cdot\cos\frac{\theta\tau}{2}S^*\left(\mu+\frac{1}{2}\theta\right)S\left(\mu-\frac{1}{2}\theta\right)d\mu\,d\tau\,d\theta\,. \tag{18}$$

We can further simplify (17) into a more meaningful form,

$$\begin{aligned}P_{\mathrm{NEW}}(t,\omega)&=\int\int\sqrt{\frac{\sigma}{4\pi\tau^2}}e^{-\frac{(\mu-t)^2}{4\tau^2/\sigma}} \cdot\frac{1}{2}\left[s(\mu+\tau)s^*(\mu)+s(\mu)s^*(\mu-\tau)\right]e^{-j\omega\tau}\,d\mu\,d\tau \qquad (19)\\ &=\frac{1}{2\pi}\int\int\sqrt{\frac{\sigma}{4\pi\theta^2}}e^{-\frac{(\eta-\omega)^2}{4\theta^2/\sigma}} \cdot\frac{1}{2}\left[S^*(\eta+\theta)S(\eta)+S^*(\eta)S(\eta-\theta)\right]e^{-j\theta t}\,d\eta\,d\theta\,. \qquad (20)\end{aligned}$$

Recall the definition of the Choi-Williams ED [1],

$$P_{\mathrm{CW}}(t,\omega)=\int\int\sqrt{\frac{\sigma}{4\pi\tau^2}}e^{-\frac{(\mu-t)^2}{4\tau^2/\sigma}}s\left(\mu+\frac{1}{2}\tau\right)s^*\left(\mu-\frac{1}{2}\tau\right)e^{-j\omega\tau}\,d\mu\,d\tau\,, \tag{21}$$

and the definition of Levin's IPS [9],

$$P_{\mathrm{IPS}}(t,\omega)=\frac{1}{2}\int\left[s(t+\tau)s^*(t)+s(t)s^*(t-\tau)\right]e^{-j\omega\tau}\,d\tau\,. \tag{22}$$

Comparing (19) with (21) and (22), we recognize immediately that the new TFD is just a combination of the Choi-Williams ED and Levin's IPS.

There is a parameter σ in the new TFD, like the one in the Choi-Williams ED and it plays the same role in both cases. In order to obtain sharp auto term resolution, σ should be larger; in order to reduce the effects of the cross terms, σ should be small. We will note soon that there should be a trade-off between auto term resolution and cross term suppression. The optimal choice of σ for a given situation needs more study, but a good choice of σ will be found in the range from 0.1 to 10, as will be shown in simulation. When σ approaches infinity, $\phi_{\mathrm{NEW}}(\theta,\tau)$ will approach $\cos(\theta\tau/2)$, so the new TFD approaches Levin's IPS, whereas the Choi-Williams ED approaches the WVD. We will conclude that the role that the new TFD plays with respect to Levin's IPS is just the counterpart of the role of Choi-Williams ED with respect to WVD.

4. Discrete form of new TFD and computer simulation

When dealing with sampled signals or digital signals, it is necessary to consider a discrete version of the TFD. The transition from the new TFD of continuous time signals to the new TFD of discrete time signals is not a trivial problem. Several cautions and approximations have to be made for this transition. This section gives the definition of the new TFD for discrete time signals and gives some computer simulations. We derive the following definition of the new TFD for discrete time signals,

$$P_{\mathrm{NEW}} = \sum_{\tau=-\infty}^{\infty} e^{-j\omega\tau} \left\{ \sum_{\mu=-\infty}^{\infty} \sqrt{\frac{\sigma}{4\pi\tau^2}} e^{-\frac{(\mu-n)^2}{4\tau^2/\sigma}} \cdot \frac{1}{2}\left[s(\mu+\tau)s^*(\mu) + s(\mu)s^*(\mu-\tau)\right] \right\} . \tag{23}$$

Compared with the ED [1] for discrete time signals,

$$P_{\mathrm{CW}}(n,\omega) = 2\sum_{\tau=-\infty}^{\infty} e^{-j2\omega\tau} \left[\sum_{\mu=-\infty}^{\infty} \sqrt{\frac{\sigma}{4\pi\tau^2}} e^{-\frac{(\mu-n)^2}{4\tau^2/\sigma}} s(\mu+\tau)s^*(\mu-\tau) \right] , \tag{24}$$

the major advantage of the new TFD over the ED for discrete time signals is

$$P_{\mathrm{NEW}}(n,\omega) = P_{\mathrm{NEW}}(n,\omega+2\pi) , \tag{25}$$

$$P_{\mathrm{CW}}(n,\omega) = P_{\mathrm{CW}}(n,\omega+\pi) . \tag{26}$$

Referring to (26), we must double the Nyquist rate to sample the continuous signal to avoid alias. Alternatively, for a real valued signal only, we can use a discrete analytic version of the signal to avoid alias instead of oversampling. However, the new TFD for a discrete time complex valued signal still does not need oversampling because its period in frequency is the sampling frequency, whereas the ED needs oversampling. Hence, the new TFD is more suitable for complex data application than the Choi-Williams ED.

For signals consisting of many samples, it is no longer possible to calculate the TFD for the complete signal. That is, for computational purposes it is necessary to apply the weighting windows $h_N(\tau)$ and $h_M(\mu)$ for summations in (26) before evaluating the new TFD at each time index n. Then, by sliding these windows along the time axis, one can obtain the running window new TFD, which is defined as follows:

$$\mathrm{RWNEW}(n,\omega) = \sum_{\tau=-\infty}^{\infty} h_N(\tau)e^{-j\omega\tau} \left\{ \sum_{\mu=-\infty}^{\infty} h_M(\mu)\sqrt{\frac{\sigma}{4\pi\tau^2}} e^{-\frac{(\mu-n)^2}{4\tau^2/\sigma}} \cdot \frac{1}{2}\left[s(\mu+\tau)s^*(\mu) + s(\mu)s^*(\mu-\tau)\right] \right\} , \tag{27}$$

where

$h_N(\tau)$ is a symmetric window, $h_N(\tau) = 0$ for $|\tau| > N/2$,
$H_M(\mu)$ is a rectangular window, $h_M(\mu) = 0$ for $|\mu| > M/2$,
$s(n)$ is the discrete analytic version of the signal.

From (27) it is clear that as long as M is large enough, RWNEW is a smoothed version of the new TFD in the frequency domain, because multiplication in the time domain corresponds to convolution in the frequency domain. That is, the parameter N, the length of the window $h_N(\tau)$, and the shape of this window determine the frequency resolution of RWNEW, whereas the parameter M and the length of the window $h_M(\mu)$ determine the range from which the time indexed autocorrelation function is to be estimated. Through experimental observations, it is found that oscillatory fluctuations of the cross terms can be reduced by decreasing the length of the window $h_N(\tau)$. On the other hand, it is also noted that the frequency resolution of the auto terms decreases as the length of the window $h_N(\tau)$ decreases. That is, the length of the window $h_N(\tau)$ determines a trade-off between the high frequency resolution of the auto terms and the smoothed cross terms.

In order to perform a real time analysis, an FFT technique can be utilized for the evaluation of RWNEW. For this purpose, one can set $\omega = 2\pi k/N$. Then (27) can be rewritten as follows:

$$\mathrm{RWNEW}(n,k) = \sum_{\tau=-\infty}^{\infty} h_N(\tau) e^{-j2\pi k\tau/N} \left\{ \sum_{\mu=-\infty}^{\infty} h_M(\mu) \sqrt{\frac{\sigma}{4\pi\tau^2}} e^{-\frac{\mu^2}{4\tau^2/\sigma}} \cdot \frac{1}{2}\left[s(n+\mu+\tau)s^*(n+\mu) + s(n+\mu)s^*(n+\mu-\tau)\right] \right\} . \tag{28}$$

We will now make some computer simulations. In simulation, we take the window functions needed in RWED, RWPTD, and IPS to all be rectangular windows with $M = 64$, $N = 64$ (PWVD is a Hamming window). Three different signals listed below are used in simulations.

Simulation 1:

$$s_1(t) = \sin\left[2\pi(0.4t + 0.7t^2)\right] + \sin[2\pi(11.6t - 0.7t^2)] .$$

Simulation 2:

$$s_2(t) = s_{20}(t) + s_{21}(t) ,$$

where

$$s_{20}(t) = \begin{cases} \sin(0.2\pi t^2) & 0 \le t \le 32 \\ 0 & \text{elsewhere,} \end{cases}$$

$$s_{21}(t) = \begin{cases} \sin[2\pi(6t + 0.2t^2)] & 11.1875 \le t \le 27.1875 \\ 0 & \text{elsewhere.} \end{cases}$$

Simulation 3:

$$s_3(t) = \sin[2\pi(0.4t + 0.6t^2)] + \sin[2\pi(0.4t + 0.8t^2)] .$$

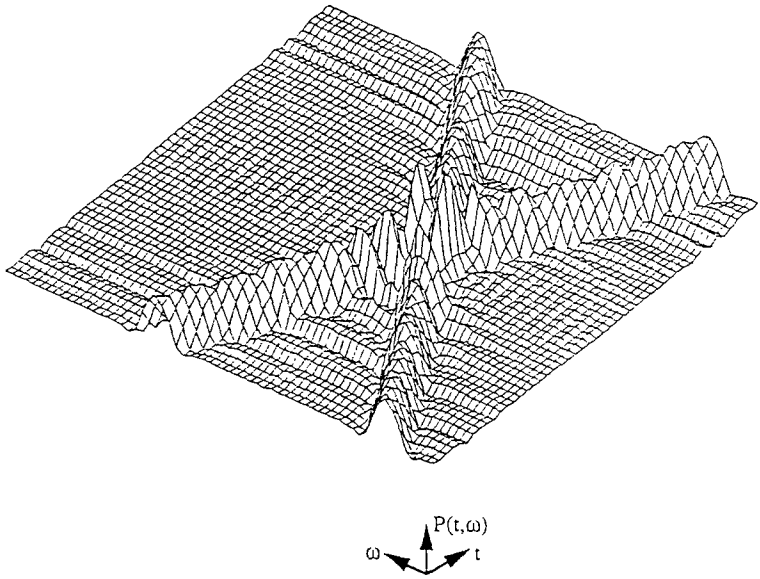

Figure 1. ED of $s_1(t)$ with $\sigma = 1$.

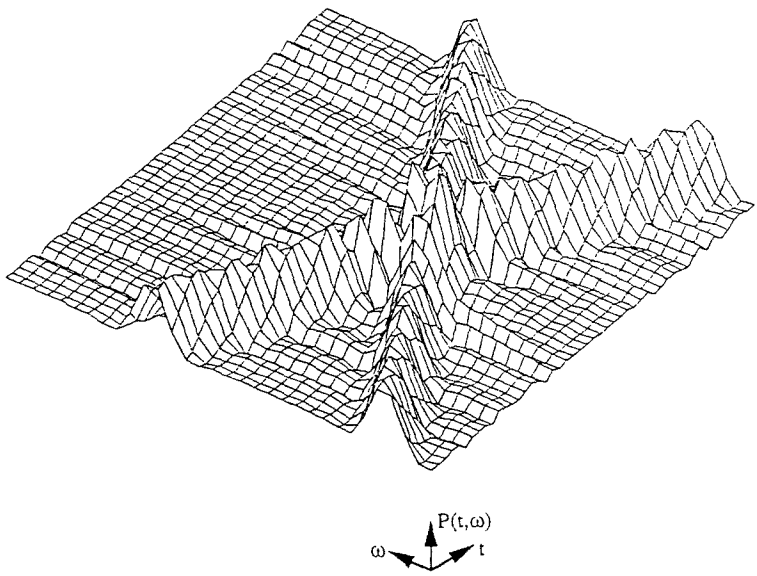

Figure 2. NTD of $s_1(t)$ with $\sigma = 1$.

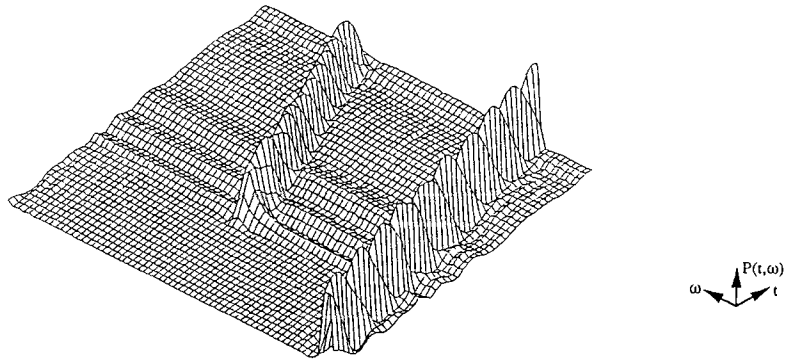

Figure 3. ED of $s_2(t)$ with $\sigma = 1$.

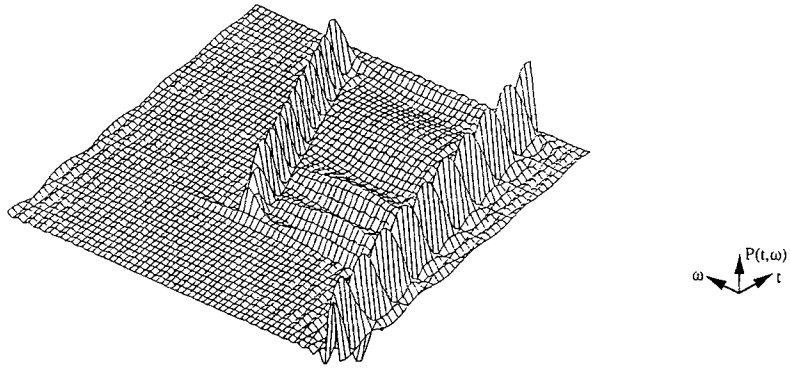

Figure 4. ED of $s_2(t)$ with $\sigma = 10$.

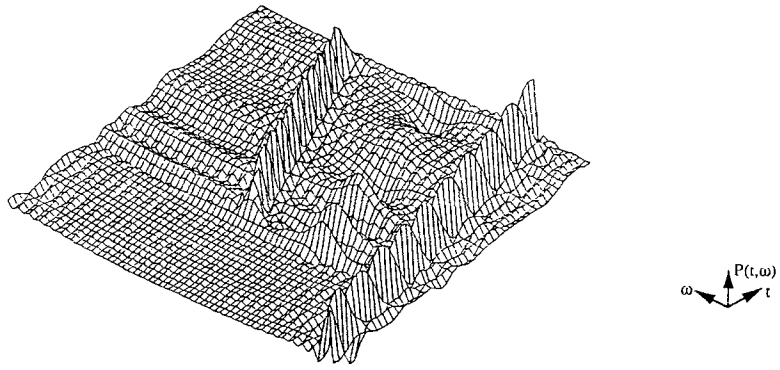

Figure 5. ED of $s_2(t)$ with $\sigma = 100$.

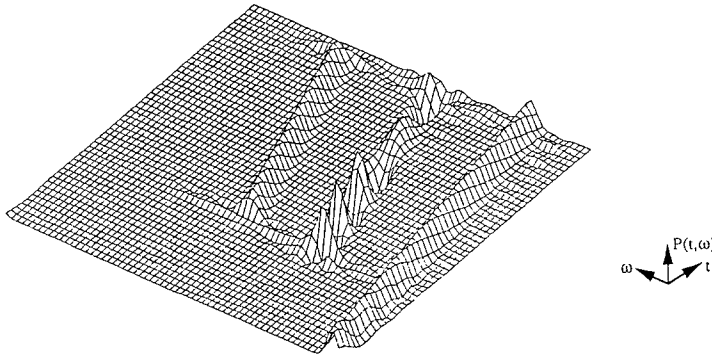

Figure 6. PWVD of $s_2(t)$ with Hamming window.

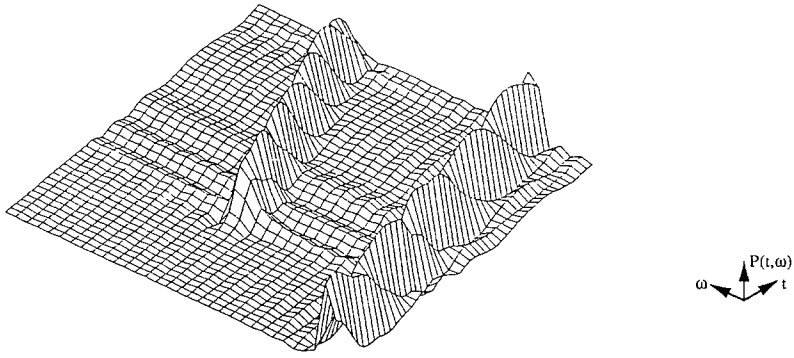

Figure 7. NTD of $s_2(t)$ with $\sigma = 1$.

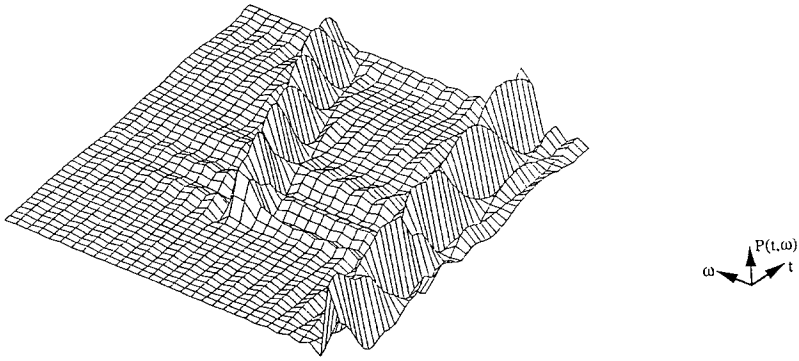

Figure 8. NTD of $s_2(t)$ with $\sigma = 10$.

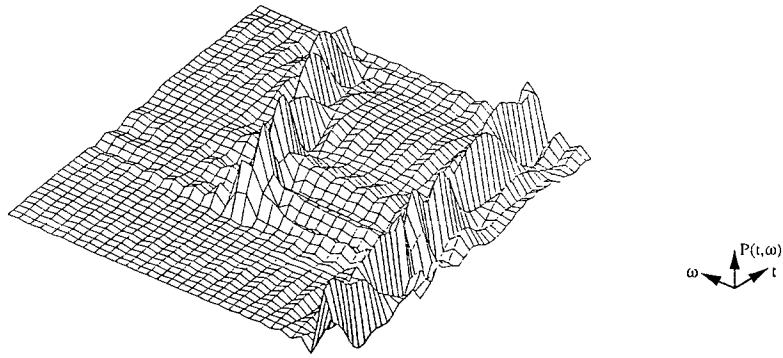

Figure 9. NTD of $s_2(t)$ with $\sigma = 100$.

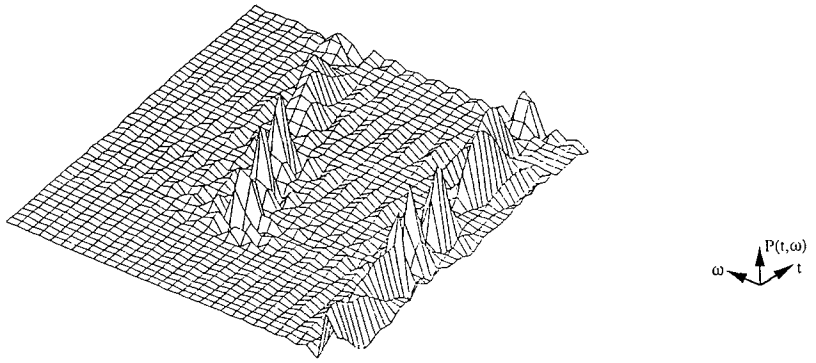

Figure 10. Levin's IPS of $s_2(t)$.

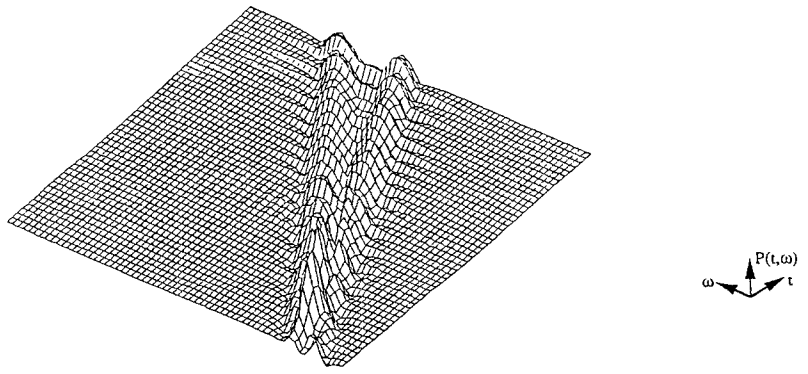

Figure 11. ED of $s_3(t)$ with $\sigma = 1$.

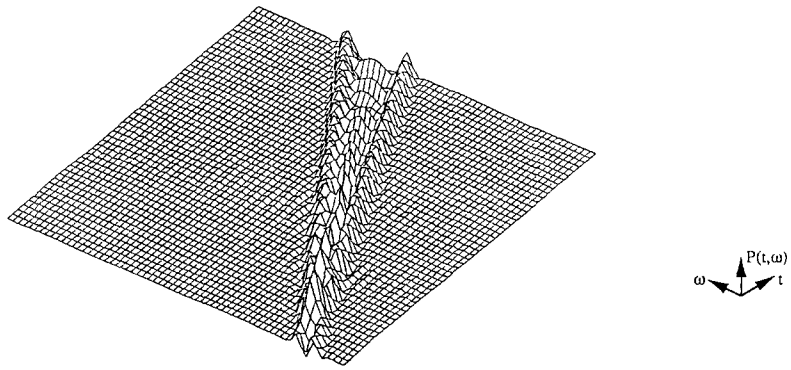

Figure 12. ED of $s_3(t)$ with $\sigma = 10$.

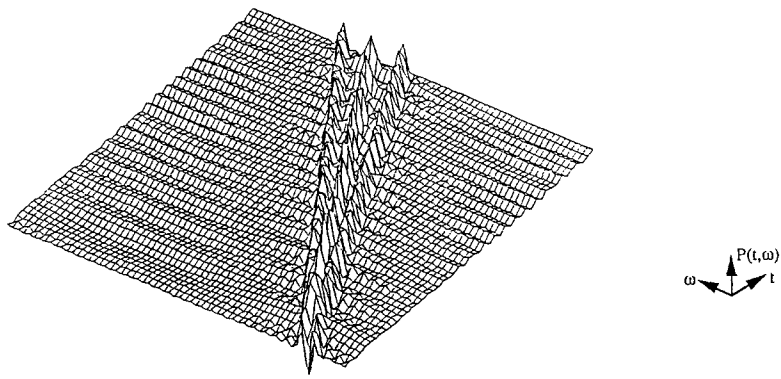

Figure 13. ED of $s_3(t)$ with $\sigma = 100$.

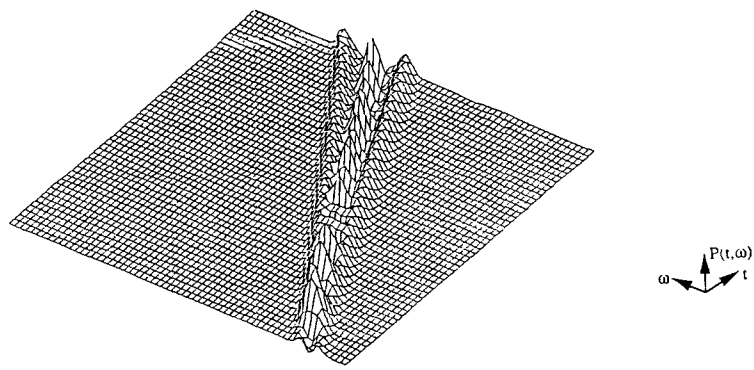

Figure 14. PWVD of $s_3(t)$ with Hamming window.

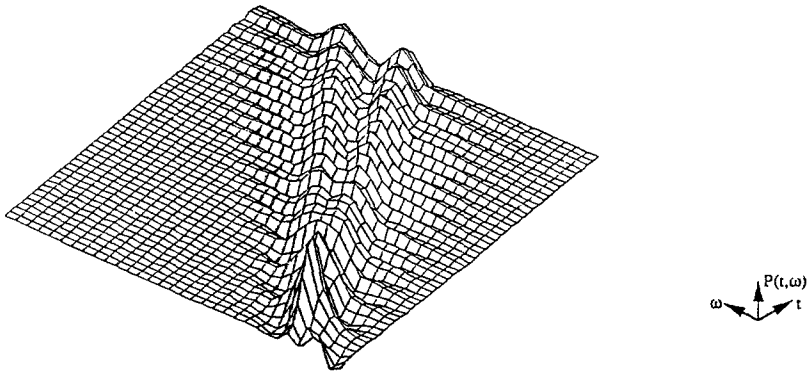

Figure 15. NTD of $s_3(t)$ with $\sigma = 1$.

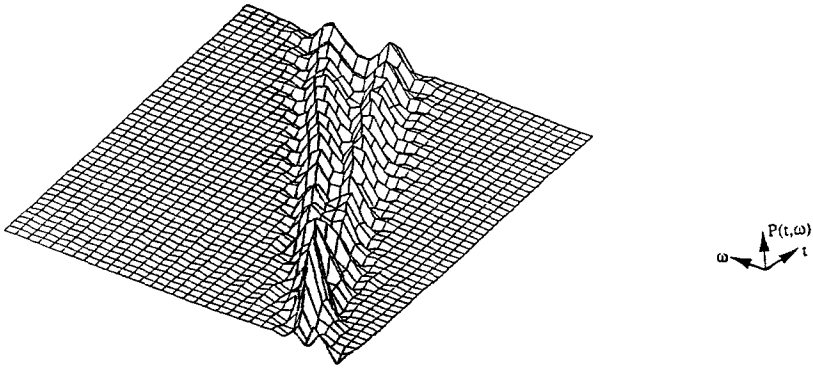

Figure 16. NTD of $s_3(t)$ with $\sigma = 10$.

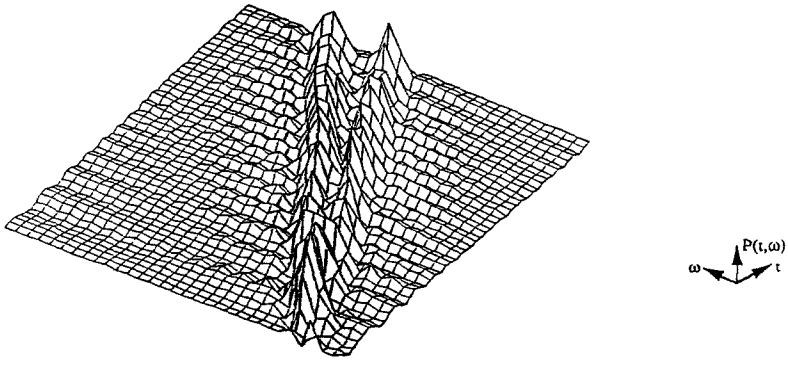

Figure 17. NTD of $s_3(t)$ with $\sigma = 100$.

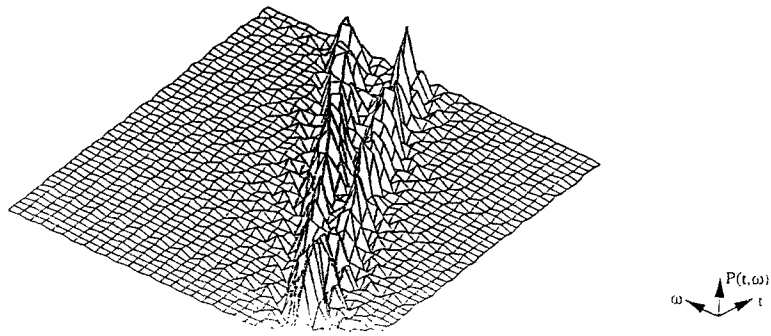

Figure 18. Levin's IPS of the $s_3(t)$.

All signals are sampled to a 512-point sequence with a 32-Hz sampling frequency. The results for the various distributions are shown in Figures 1 through 18. From these figures, we will clearly observe the role σ plays in determining cross term attenuation and auto term sharpness in the ED and the new TFD. We make the following conclusions:

(1) If σ is small, the order of σ is about 1: Kernels of both the ED and new TFD will attenuate cross terms effectively, so both distributions look similar and the new TFD's cross term concentration property is of a minor benefit. However, the smaller σ is, the more the auto terms of both distributions spread.

(2) IF σ is large, the order of σ is about 10: The auto terms of both distributions become sharper than for small σ, while providing cross term attenuation in return. In the ED, cross terms will appear obvious gradually, but in the new TFD, cross terms will be still under control because of the cross term concentration property.

(3) IF σ approaches infinity, the order of σ is about 100: The ED will approach WVD, and the TFD will approach Levin's IPS.

5. Conclusion

A Time-Frequency Distribution (TFD) is a powerful tool for analyzing time-varying signals. However, the cross term effect due to the second order form of Cohen's class severely blocks its application. In this paper we have promoted a new TFD that not only meets several useful TFD requirements but also has good interference immunity. We have also induced that the new TFD plays a role with respect to Levin's IPS that is a counterpart of the one that the Choi-Williams ED plays with respect to the WVD.

References

[1] H.I. Choi and W.J. Williams, Improved time frequency representation of multicomponent signals using exponential kernels, *IEEE Trans. on A.S.S.P.*, vol. 37, pp. 862–871, 1989.

[2] T.A.C.M. Classen and W.F.G. Mecklenbrauker, The Wigner distribution — A tool for time frequency signal analysis; Part 1: Continuous time signals, *Philips J. Res.*, vol. 35, pp. 217–250, 1980.

[3] T.A.C.M. Classen and W.F.G. Mecklenbrauker, The Wigner distribution — A tool for time frequency signal analysis; Part 2: Discrete time signals, *Philips J. Res.*, vol. 35, pp. 276–300, 1980.

[4] T.A.C.M. Classen and W.F.G. Mecklenbrauker, The Wigner distribution — A tool for time frequency signal analysis; Part 3: Relations with other time frequency signal transformations, *Philips J. Res.*, vol. 35, pp. 372–389, 1980.

[5] L. Cohen, Generalized phase space distribution function, *J. Math. Phys.*, vol. 7, pp. 781–786, 1966.

[6] L. Cohen, Time frequency distribution — A review, *IEEE Proc.*, vol. 77, pp. 941–981, 1989.

[7] P. Flandrin, Some features of time frequency representations of multicomponent signal, *IEEE Intl. Conf. on A.S.S.P.*, vol. 3, pp. 41B.4.1–41B.4.4, 1984.

[8] J.G. Kirkwood, Quantum statics of almost classical ensembles, *Phys. Rev.*, vol. 44, pp. 31–37, 1933.

[9] M.J. Levin, Instantaneous spectra and ambiguity function, *IEEE Trans. on Informat. Theory*, vol. 13, pp. 95–97, 1967.

[10] P.J. Loughlin, J.W. Pitton, and L.E. Atlas, New properties to alleviate interference in time-frequency representations, *IEEE Intl. Conf. on A.S.S.P.*, vol. 5, pp. 3205–3208, 1991.

[11] C.H. Page, Instantaneous power spectra, *J. Appl. Phys,.*, vol. 23, pp. 103–106, 1952.

[12] J. Ville, Theorie et applications de la notion de signal analytique, *Cables et transmission*, vol. 2A, pp. 61–74, 1948.